Moisture Diffusivity of Fiber Reinforced Silica Fume Mortars

By E. Denarié and Y.F. Houst

Synopsis **:** The moisture diffusivity is of considerable importance for quantitative assessments of creep and shrinkage as well as durability of cementitious material. For this reason, the influence of the composition of repair mortars on their effective moisture diffusivity as a function of the relative humidity of the surrounding air has been investigated. Silica fume, superplasticizer and polypropylene fibers have been added in order to reduce the permeability and to control cracking induced by drying shrinkage. It has been shown that the moisture transport in cementitious materials can be realistically described by a non-linear diffusion process governed by Fick's law. A computer program based on the finite volume method has been used in order to get the best effective moisture diffusivity by comparing experimental results (moisture losses of drying mortar cylinders) with the numerical solution. The applicability of a combined experimental-numerical approach to characterize repair mortars regarding their moisture diffusivity has been demonstrated. The material properties necessary for the characterization and qualification of new materials can be found numerically. Moreover, the diffusivities obtained provide useful input data for further numerical calculations. The positive effect of the addition of silica fume on the moisture diffusivity was clearly shown. The positive combined effect of polypropylene fibers and silica fume with increasing entrained air content was observed. Finally, no significant detrimental effect on the addition of fibers (even at relatively high volumes) has been observed for materials cast under shrinkage free conditions.

Keywords: Repair Mortars, Silica Fume, Polypropylene Fibers, Moisture Diffusivity, Numerical Simulation, Drying, Transition Zone.

Denarié E. and Houst Y.F., Moisture Diffusivity of Fiber Reinforced Silica Fume Mortars, **in** Fly Ash, Silica Fume, Slag and Natural Pozzolans in Concrete. Proceedings Fifth International Conference, Milwaukee, Wisconsin, USA 1995. (Malhotra V.M. Ed.), SP 153-40, American Concrete Institute, Detroit, 1995, Vol. 2, pp. 763-777.

Emmanuel Denarié, a civil engineer, is research engineer at the Laboratory for Building Materials, Federal Institute of Technology, Lausanne, Switzerland. He is currently working on the development of new testing methods for fiber reinforced cementitious materials.

ACI member Yves F. Houst, a chemist, dr. ès sciences, is the Head of the *Cement Group* of the Laboratory for Powder Technology, Federal Institute of Technology, Lausanne, Switzerland (EPFL). He is involved in various research programs related to properties of cement, suspensions, admixtures and durability of cementitious materials. He is also a lecturer at the EPFL.

INTRODUCTION

The number of defects detected on concrete surfaces in buildings or highway bridges has increased dramatically in the last few years. Most often, these defects are due to spalling of the concrete cover produced by the corrosion of the reinforcement. As a consequence, the demand for repair mortars able to restore the protection of the reinforcement and give a second life to the damaged structures is growing significantly. The properties required for these materials are somewhat contradictory such as a very high compactness (to limit the penetration of aggressive substances like water, CO_2, O_2, chlorides..) and at the same time the ability to withstand thermal stresses and to provide sufficient bonding to the old concrete without cracking (which means for instance a low elastic modulus, i.e. a good strain compatibility with the base concrete).

Beside the use of polymer modified mortars, the addition of very fine pozzolanic-fillers such as silica fume has proven to be highly efficient in reducing the moisture diffusivity and the penetration of dangerous substances.

It has been shown in a previous study (1) that tensile stresses higher than the intrinsic strength of the material could appear in the neighborhood of the concrete-mortar interface, depending on drying conditions. In that same study, it was also shown that the first week after the application of a repair mortar, is critical for the risk of cracking due to drying shrinkage. Thus, the curing conditions are particularly important and the drying shrinkage is partially dependent on the moisture diffusivity.

From the law of mixtures, one possible solution to decrease the elastic modulus and thus increase the elasticity is to add low or zero modulus materials such as entrained air or polypropylene fibers. Unfortunately, due to the relatively low quantities that can be added to normal mortars, the fibers cannot contribute in a significant way to the decrease of the elastic modulus. Nevertheless, synthetic fibers are known to act as a reinforcement of the microstructure of the cement paste at early ages by preventing and distributing internal stresses (due to plastic shrinkage, to bleeding, etc.), thus decreasing the permeability of concrete surfaces.

Consequently, it appears that a suitable mix for repair mortars could be sought in the mixture of silica fume + synthetic fibers + entrained air.

The aim of this study was to investigate the effect of the addition of silica fume with or without synthetic fibers on the moisture diffusivity for several repair mortars including air-entrained ones. It is part of an ongoing research program on repair mortars for concrete (1, 2).

MOISTURE DIFFUSION IN CEMENTITIOUS MATERIALS

Theory

In cementitious materials, there is continuous transfer in the form of water vapor and condensed water. The transport of liquid water is slow enough to be purely laminar and can be described by Hagen-Poiseuille's law. In the general case, the porous materials are not saturated and several mechanisms can take place simultaneously. If the pore dimensions are smaller than the mean free path[1] of water molecules, Knudsen's diffusion takes place. In larger pores, where the mean free path of gas molecules is smaller than the pore diameter, normal gas diffusion predominates. In pores of intermediate size, Knudsen and normal diffusion occur at the same time. In addition to these two mechanisms, surface diffusion also can occur at the same time. But, there are some indications that surface diffusion is a mechanism of only secondary importance in inorganic building materials (3).

Despite the complicated transport mechanisms which occur in materials such as cement paste or mortar, moisture diffusion can be described by Fick's second law which describes the continuity of the moisture flow through an infinitely small material layer. In the unidirectional case with w being the local water content and D(w) the corresponding effective diffusion coefficient or diffusivity, one gets:

$$\frac{\partial w}{\partial t} = \frac{\partial}{\partial x}\left(D(w)\frac{\partial w}{\partial x}\right) \qquad (1)$$

The diffusivity D is an unknown function of the water content w and thus equation (1) has to be solved numerically in the general case.

For concrete-like materials, the diffusivity can be dramatically modified by the porosity (size and distribution of the pores and of the microcracks) of the cement paste and of the interfacial zones. The addition of silica fume reduces the porosity in several ways. Firstly, the silica particles are on average ten to twenty times smaller than the cement grains and thus they extend the particle size distribution of cement in the range of very fine grains providing a better geometrical packing. Secondly, their very high specific surface (almost one hundred times that of cement) and their high content in amorphous SiO_2 make them a very reactive pozzolan. Finally, these two effects are combined during the formation of the microstructure of hydrated cement paste (hcp), where the

[1] The distance a molecule travels between collisions. This distance is $1.7 \cdot 10^{-7}$ m at 20°C and 1 atm for a water molecule.

pozzolanic reaction fills voids with dense C-S-H gel and consumes the porous calcium hydroxide.

Synthetic fibers such as polypropylene have a lower elastic modulus than hcp. For this reason, their action on the control and redistribution of internal stresses is mostly limited to early ages, when their modulus is still higher than that of the cementitious matrix. Nevertheless, many phenomena such as plastic shrinkage, bleeding, autogeneous shrinkage, occur during this period which can dramatically influence the physical and mechanical properties of the material surface and especially the moisture diffusivity. Provided that the specimens are submitted to restrained shrinkage, several authors have shown the positive effect of polypropylene fibers on the crack distribution and width (4).

Numerical Simulation

Various forms of the diffusivity have been found to be realistic; for instance the exponential type used by Mensi et al (5), described by two parameters or the S shape type from Bazant and Najjar (6) which better describes the moisture flow at high water contents but includes four parameters.

One possible approach to get an estimation of the diffusion coefficient is to use a numerical simulation of drying experiments where D(w) is assumed to follow a simple function (for instance exponential) completely defined by a set of parameters (p_1, p_2,...). These parameters are determined by fitting the numerical drying results to the measured drying data (7). The best fit is obtained by successive iterations.

The code used for the simulation of the drying experiments was developed by Sadouki (8). It calculates, by means of the finite volume method, the drying of cylindrical specimens with any boundary conditions. In this case, the perimeter of the cores was sealed and drying occurred only uniaxially.

The transport driving force is input by means of the initial water content (at saturated state) w_0 and the final water content (at equilibrium with the external relative humidity RH) w_b.

w_b was determined through extrapolation of the experimental drying curves (by fitting to a bi-hyperbolic function of time, see 4.2). The diffusion coefficient can be any differentiable function. For this simulation, the following function was chosen:

$$D(w) = p_1 \exp(p_2 \frac{w}{w_o}) \qquad (2)$$

EXPERIMENTAL

Materials

Normal portland cement (PC) from the plant at Eclépens (Switzerland) was of ASTM C150 type I, with fineness defined by specific surface area 290 m^2/kg (Blaine). The silica fume (SF) was imported from Germany[2] in a gray powder form slightly densified. The silica content was 96.5 % of amorphous silica, the BET specific surface area was 20'000 to 22'000 m^2/kg, and the density 2'200 kg/m^3.

The sand (0-3 mm) from a glacial moraine was composed of 80 % of rounded shape particles and 20 % crushed. Mineralogically, this sand was composed of 40 to 46 % calcite, 29 to 32 % quartz, 8 to 13 % residue of crystalline rocks of multimineral composition, predominantly quartzitic, and 12 to 18 % of composite grains, essentially quartzitic. The grading curve of the sand was already given in (2).

For all the mortars, one superplasticizer[3], consisting of sulfonated melamine formaldehyde condensate, has been used. For certain mortars, one air-entraining admixture[4] , has also been used.

The collated fibrillated polypropylene fibers[5] were 19 mm long. The density was 920 kg/m^3, the elastic modulus was 5 GPa and the tensile strength at least 0.5 GPa.

Mortars

The cement content of the mortars varied from 468 to 556 kg/m^3 with C+SF ranging from 515 to 556 kg/m^3. W/(C+SF) was kept constant at 0.41 and C/A at 0.37 to 0.38 (W, C, SF and A being respectively the water, cement, silica fume and aggregate content by mass). The consistency, defined by the spread value, was about the same, i.e. between 120 and 150 mm. The composition of the mortars is given in Table 1. Nine different mortars were prepared. The mortars 1 to 3 contained 10 % silica fume relative to the mass of cement. These mortars differed only from one another in the quantity of the superplasticizer and the air-entraining admixture. The mortars 4 to 6 had the same composition as the mortars 1 to 3, except a fiber content of 0.1 % by volume. The mortars 7 to 9 do not contain any silica fume. In order to keep the volume of binder constant, the silica fume was replaced by an equivalent volume of cement. The fiber content was varied from 0 to 0.6 % by volume (which is the practical limit from the point of view of the workability of the fresh mix for this type of fiber). It was not possible to increase this amount and maintain a constant consistency. The consistency of these mortars was regulated by using the superplasticizer only.

---

[2] Trademark: V.A.W. RW Füller.
[3] Trademark: Sikament 320.
[4] Trademark: Sika Fro V5.
[5] Trademark: Forta, type A5.

The binder content was chosen according to Caquot's formula[6], which relates the minimum cement content to the maximum grain size of the aggregate, necessary to give a compact mortar or concrete. For a D_{max} of 3 mm, the calculated minimum cement content C_{min} is 482 kg/m^3.

The total mass of ingredients for a batch was 26.7 kg. The preparation of a fiber reinforced mortar was carried as follows:

- mixing of sand, cement, and silica fume if used, for 2 min.
- addition of water.
- addition of admixtures.
- addition of fibers (if needed) and final mixing for 3 to 7 min, depending on the fiber content.

The mortars were cast into molds to prepare slabs 500x400x40 mm^3. The slabs were cured at RH > 95 % and 20°C for 28 days. The slabs were free to deform (except for friction at the mold surfaces), in order to test the pure material behavior of the mortars independently of the structural related cracking due to restrained shrinkage. The aim was to evaluate the possible detrimental effect of the fibers added as an inclusion on the diffusivity and see how it was affected by the addition of silica fume and/or entrained air.

Physical and Mechanical Properties of the Mortars

The bulk density of the fresh mortar was calculated after having measured the mass of one liter of mortar.

The air content was measured by the pressure method which allowed us, after calibration of the apparatus, to read the percentage of air directly.

The consistency of the mortar was measured with a flow table in accordance with Swiss Standard SIA 115. This equipment is close to that described in ASTM Standard C 230. The mean diameter of the mortar specimen measured in two perpendicular positions, after it has been spread by the operation of the table, represents the spread value.

Three prisms 40x40x160 mm^3, which had been sawn from the slabs, were used to determine the flexural strength. They were tested in 3 points bending with a span of 100 mm. After the tests, the two parts of the prisms were used for the determination of the compressive strength.

Drying Experiments

For these experiments, cores of mortars of 50 mm diameter and 38 mm length drilled from the slabs were used. Then, these cores were saturated with water under vacuum and their mass measured by weighing. The cores were placed into synthetic rubber tubes so that the cylinders of mortar could dry only axially.

---

[6] $C_{min} = \frac{600}{\sqrt[5]{D_{max}}}$

They were immediately transferred into a glove box at 55 % RH and 20°C. The mass of the specimens was recorded as a function of time. After the measurements, the tubes were removed and the cylinders of mortar dried at 105°C and weighed in order to calculate their maximum water content, i.e. their open porosity which corresponds to water saturation data.

RESULTS AND DISCUSSION

Physical and Mechanical Properties

The compressive and flexural strengths as well as the bulk densities are given in Table 1.

The addition of fibers has only a slightly detrimental effect on the flexural strength. This is probably due to additional defects introduced by the air-entraining admixture together with fibers.

The adjunction of entrained air at high content decreases in a significant way the compressive strength (mortars 1, 2, 3 and 4, 5, 6), but not the flexural strength. This could be expected as the flexural strength is mostly determined by a very small zone where stresses are maximum (outer border of the specimen), the compressive strength however is measured on almost the whole volume of the specimen.

The positive effect of silica fume on compressive and flexural strengths is all the same very clear as expected.

Drying Curves

The drying of 4 specimens of each mortar has been recorded as a function of time. The results are represented graphically in Fig. 1 to 5. Each experimental point of the curve is the mean value of 4 measurements. In order to estimate the asymptotic value of the water loss, which is required as an input value for the numerical simulation, the following function was fitted to experimental data:

$$\frac{\Delta m}{m} = \frac{a_1 t}{a_2 + t} + \frac{a_3 t}{a_4 + t} \qquad (3)$$

were $\Delta m/m$ is the water loss, t the time and a_1, a_2, a_3, a_4 parameters. The sum of parameters a_1 and a_3 is equal to the final water loss ($t=\infty$), i.e. the equilibrium water content. The parameters a_1 to a_4 are given in table 2 and the corresponding calculated curves are represented by solid lines in Fig. 1 to 5.

The presence of fibers always reduces the water loss as a function of time. That means that the evaporable water at 55% RH of saturated mortars, the sum of a_1 and a_3, is always lower for mortars with fibers (Fig. 1 and 2). The effect of silica fume is the same with or without fibers (Fig. 3 and 4). The evaporable water of mortar 1 (with silica fume) is hardly higher than that of mortar 7 (without silica fume). This could be an inaccuracy due to the extrapolation of the asymptote of

the drying curve. On the other hand, one can see that the bi-hyperbolic function of equation 3, represented by solid lines in Fig. 1 to 5, fits the experimental data very well. This indicates that the choice of the function, which is purely empirical, was adequate. Therefore, a better evaluation of the asymptotic value could be obtained by measuring the drying loss for a longer time.

Diffusivity

The diffusivity was obtained by means of numerical simulation of the drying experiment. The fit was performed iteratively by slightly changing the parameters p_1 and p_2 of the diffusivity function, until a satisfactory visual matching of the numerical results with the experimental data was reached. The procedure was the same for the nine mortars. An example of a typical fit obtained is given in Fig. 6.

Table 3 summarizes the values of the parameters p_1 and p_2 which gave the closest fit while Fig. 7 shows the diffusivity obtained by the numerical simulation for all the mortars tested.

From these curves, several trends can be distinguished. First, the addition of silica fume has a marked effect in reducing the diffusivity for all the mixes. Secondly, the addition of fibers together with silica fume shows very small (mortars 1 and 4) or no differences (mortars 2 and 5) in the moisture diffusivity of zero to medium content of entrained air. Conversely, a maximum effect in the case of the highest content of entrained air (mortar 3 and 6) is observed. In fact, with increasing entrained air content, the effect of the addition of fibers together with silica fume on the diffusivity changes gradually from slightly detrimental to no effect and finally a very clear positive effect, even providing the lowest diffusion coefficient of all the tested mixes. This effect cannot be explained by existing results. Further investigations are necessary to confirm this trend.

Finally, the effect of the addition of fibers to mortars without silica fume is slightly detrimental on the diffusivity. More important, no difference can be observed between the usual fiber content (0.1 vol. %) and the maximal one (0.6 vol. %). This tends to suggest that the difference is more likely to come from the mixing and casting operations, which are less easy with high fiber content, than from a detrimental effect of the supplementary interfacial zones introduced by the fibers.

CONCLUSIONS

In this study, the applicability of a combined experimental-numerical approach to characterize repair mortars regarding their diffusivity has been demonstrated.

Besides standard drying experiments, the numerical simulation enables one to determine a diffusivity by fitting calculated drying results to the experimental data. In this way, the material properties necessary for the characterization and qualification of new materials can be found numerically.

Moreover, the diffusivities obtained provide useful input data for further numerical calculations.

The positive effect of the addition of silica fume on the moisture diffusivity was clearly shown.

The positive combined effect of polypropylene fibers and silica fume with increasing entrained air content was observed.

Finally, no significant detrimental effect of the addition of fibers (even at relatively high volumes) has been observed for materials cast under shrinkage free conditions.

REFERENCES

1. Jaquerod, C., Alou, F., and Houst Y.F. " Nondestructive testing of Repair Mortars for Concrete", Proceedings of the 3rd International Colloquium on Materials Science and Restoration, (F.H. Wittmann, Ed.), Expert Verlag, 1993, Vol. 1, pp. 872-888.

2. Alou, F., and Houst, Y.F. " Repair Mortars for Concrete Exposed to Freeze-Thaw and Deicer Salts", 4th CANMET/ACI International Conference on Fly Ash, Silica Fume, Slag and Natural Pozzolans in Concrete", Istanbul, Turkey, 1992, Supplementary Papers, pp. 331-350.

3. Quenard, D., and Sallée, H. "Water Vapour Adsorption and Transfer in Cement-Based Materials: a Network Simulation", Materials and Structures, Vol. 25, 1992, pp. 515-522.

4. Bentur, A., and Mindess, S. "Fiber Reinforced Cementitious Composites", Elsevier Applied Science, London and New-York, 1990, pp. 334.

5. Mensi, R., Acker, P., and Attolou, A. " Séchage du béton: analyse et modélisation", Materials and Structure, Vol. 21, 1988, pp. 3-12.

6. Bazant, Z.P., and Najjar, L.J. "Non Linear Water Diffusion in Non Saturated Concrete", Materials and Structures, Vol. 5, Number 25, 1972, pp. 3-20.

7. Wittmann, X., Sadouki, H., and Wittmann F.H. "Numerical Evaluation of Drying Test Data", Trans. 10th SMIRT (A.H. Hadjan, Ed.), Anaheim, CA, USA, 1989, Vol. H, pp. 71-79.

8. Sadouki, H., Personal Communication, 1994.

ACKNOWLEDGMENT

The authors wish to thank dr. H. Sadouki for having provided them with a part of his computer code and for his valuable advice on numerical problems.

Table 1 - Composition and characteristics of the mortars.

Mortar No	**1**	**2**	**3**
Sand [kg/m^3]	1443	1421	1405
Cement [kg/m^3]	481	474	468
Silica fume [kg/m^3]	48	47	47
Water [kg/m^3]	216	213	211
Superplasticizer [kg/m^3]	12	8	7
Air-entr. adm. [kg/m^3]	0	1	2
Fibers [L/m^3]	0	0	0
Bulk dens. [kg/m^3]	2200	2164	2140
Air [vol. %]	6.4	8.0	8.9
Spread [mm]	140	140	140
W/(C + SF)	0.41	0.41	0.41
C. strength [MPa]*	59.2	56.0	49.2
F. strength [MPa]**	9.7	9.7	8.4

Mortar No	**4**	**5**	**6**
Sand [kg/m^3]	1443	1421	1405
Cement [kg/m^3]	481	474	468
Silica fume [kg/m^3]	48	47	47
Water [kg/m^3]	216	213	211
Superplasticizer [kg/m^3]	12	8	7
Air-entr. adm. [kg/m^3]	0	1	2
Fibers [L/m^3]	1	1	1
Bulk dens. [kg/m^3]	2201	2165	2141
Air [vol. %]	6.4	7.9	8.9
Spread [mm]	135	135	135
W/(C + SF)	0.41	0.41	0.41
C. strength [MPa]*	62.2	59.2	50.7
F. strength [MPa]**	9.0	9.3	9.1

Mortar No	**7**	**8**	**9**
Sand [kg/m^3]	1444	1445	1464
Cement [kg/m^3]	549	549	556
Silica fume [kg/m^3]	0	0	0
Water [kg/m^3]	225	225	228
Superplasticizer [kg/m^3]	6	10	15
Air-entr. adm. [kg/m^3]	0	0	0
Fibers [L/m^3]	0	1	6
Bulk dens. [kg/m^3]	2220	2230	2270
Air [vol. %]	5.8	5.4	3.3
Spread [mm]	145	150	120
W/(C + SF)	0.41	0.41	0.41
C. strength [MPa]**	51.9	52.0	55.5
F. strength [MPa]**	6.7	6.2	5.7
* Test performed at 14 days		** Test performed at 28 days	

Table 2 - Parameters a_1 to a_4 obtained by fitting equation 3 to experimental data.

Mortar No	**1**	**2**	**3**	**4**	**5**	**6**	**7**	**8**	**9**
a_1	4.41	1.41	7.09	3.10	3.83	1.83	1.20	1.51	4.40
a_2	58.10	0.82	61.34	43.58	50.72	1.31	1.04	0.89	24.23
a_3	1.33	4.96	2.60	1.06	1.26	7.39	4.22	4.71	1.50
a_4	0.890	59.72	1.91	0.680	0.800	65.68	30.57	28.78	0.887

Table 3 - Parameters p_1 and p_2 of equation 2 obtained by fitting of the numerical results to measured drying data.

Mortar No	**1**	**2**	**3**	**4**	**5**
p_1 [m^2/s]	$3.61 \cdot 10^{-12}$	$5.09 \cdot 10^{-12}$	$6.36 \cdot 10^{-12}$	$3.47 \cdot 10^{-12}$	$5.09 \cdot 10^{-12}$
p_2 [-]	4.4	4.0	4.1	4.5	4.0

Mortar No	**6**	**7**	**8**	**9**
p_1 [m^2/s]	$6.36 \cdot 10^{-12}$	$1.04 \cdot 10^{-11}$	$1.27 \cdot 10^{-11}$	$1.27 \cdot 10^{-11}$
p_2 [-]	3.7	4.0	4.0	4.0

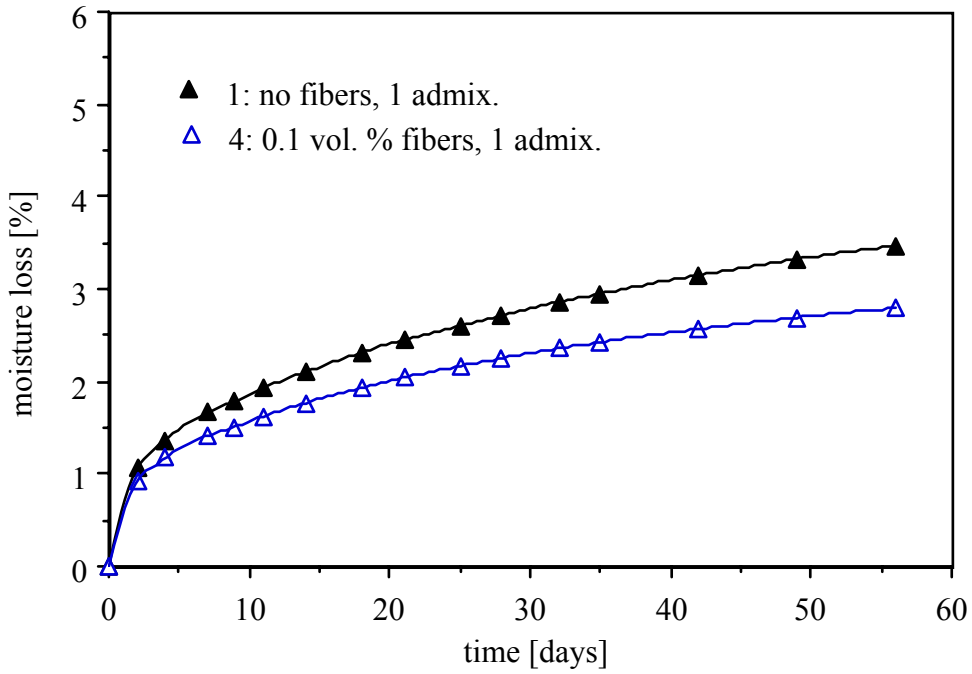

Fig. 1 - Drying curves of mortars 1 and 4. The solid line was fitted using equation 3.

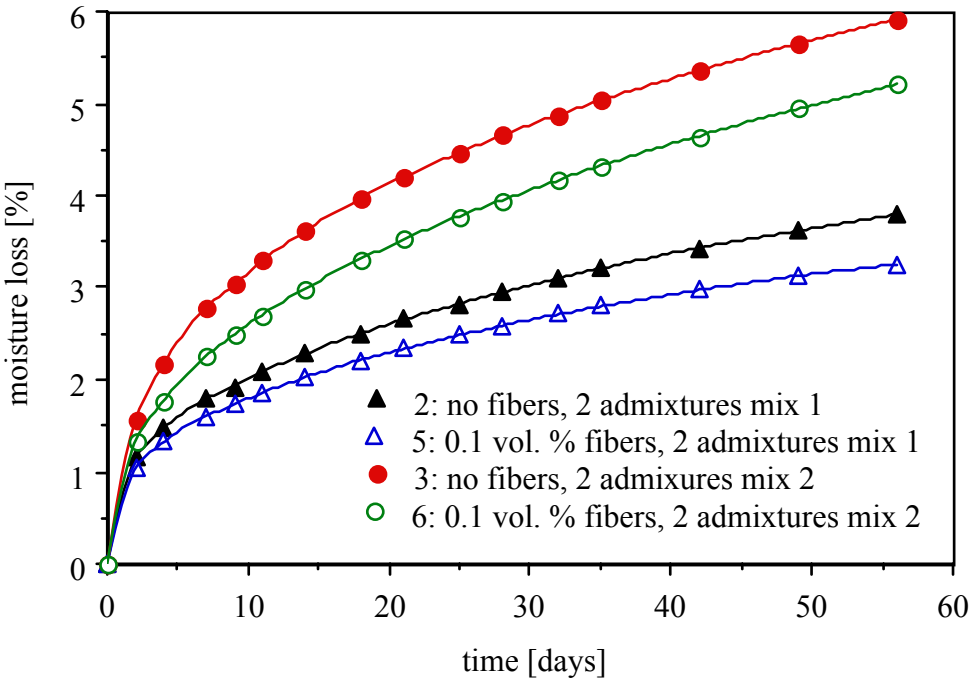

Fig. 2 - Drying curves of mortars 2, 3, 5 and 6. The solid line was fitted using equation 3.

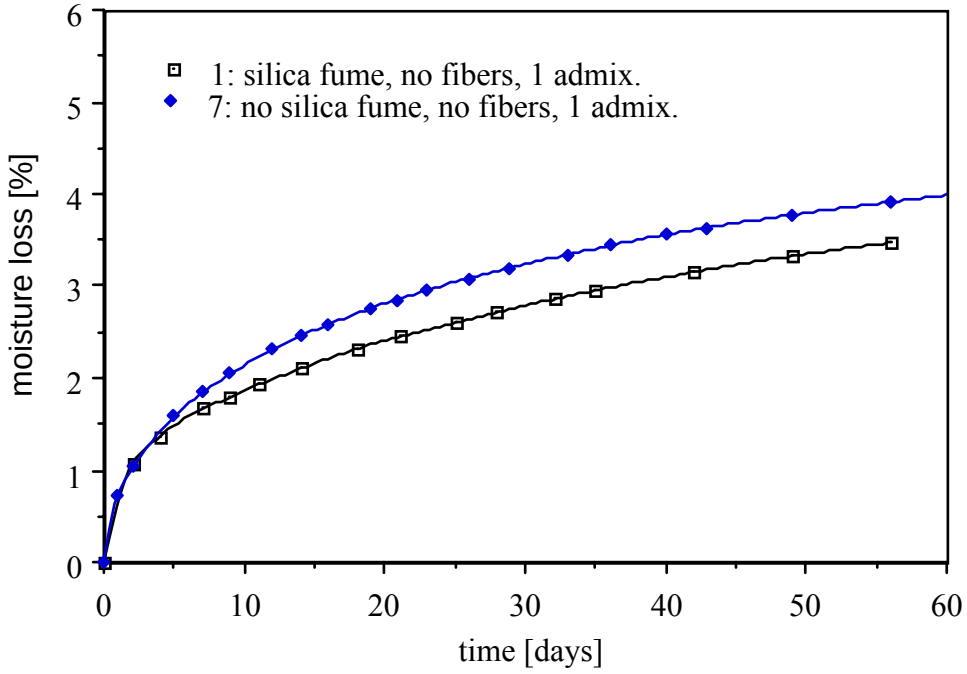

Fig. 3 - Drying curves of mortars 1 and 7. The solid line was fitted using equation 3.

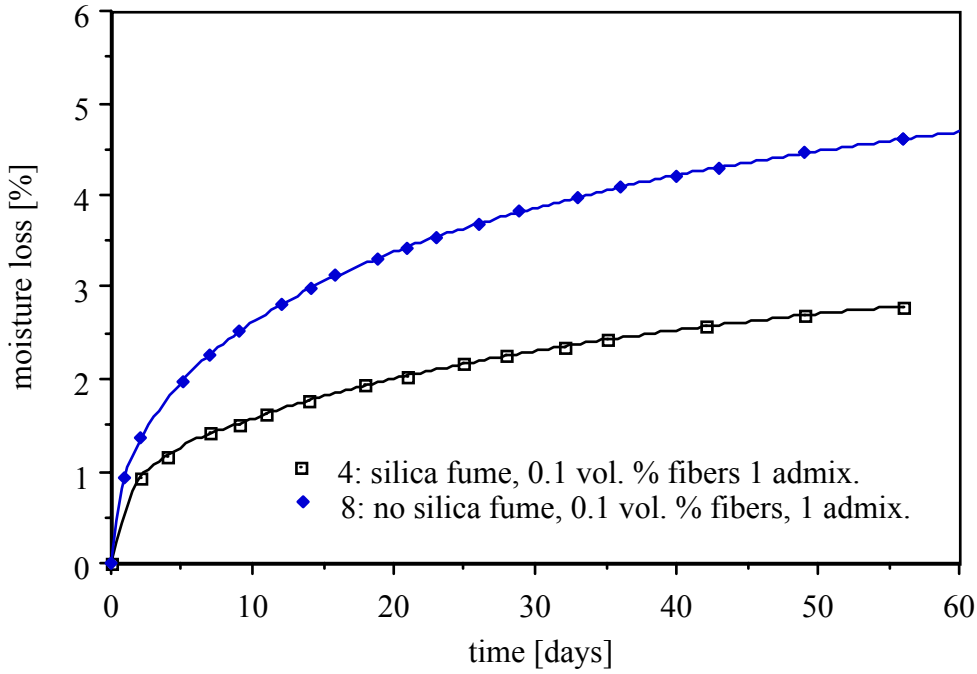

Fig. 4 - Drying curves of mortars 4 and 8. The solid line was fitted using equation 3.

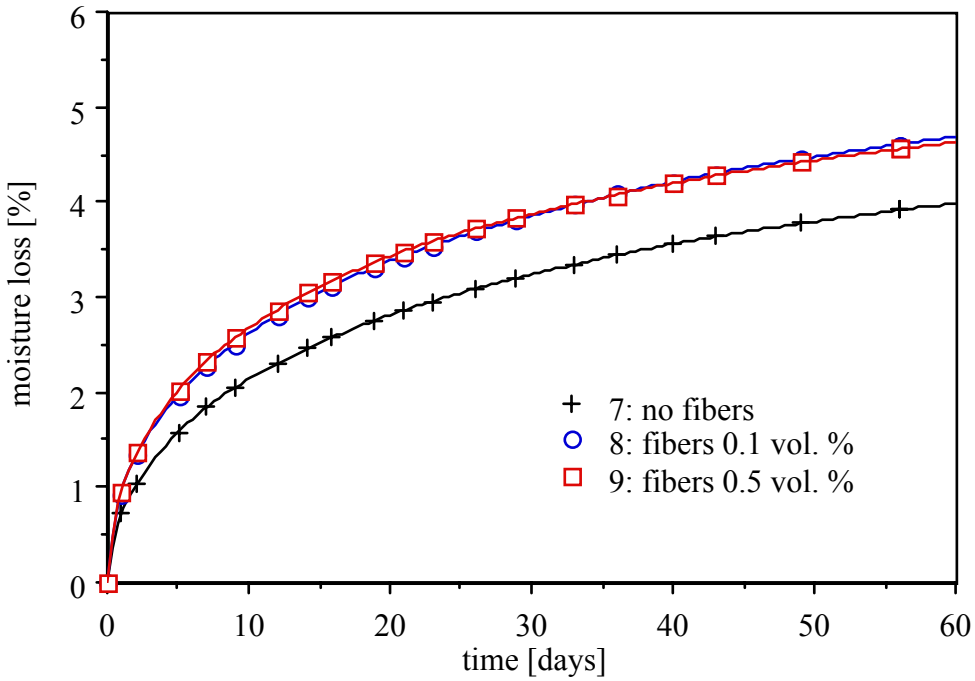

Fig. 5 - Drying curves of mortars 7, 8 and 9. The solid line was fitted using equation 3.

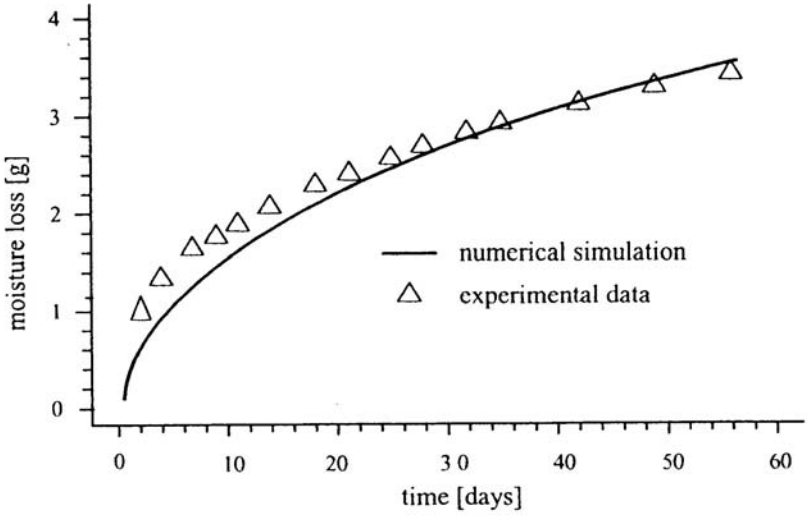

Fig. 6 - Moisture loss as a function of time for mortar 1. The solid line was fitted and corresponds to the best fit obtained by numerical simulation.

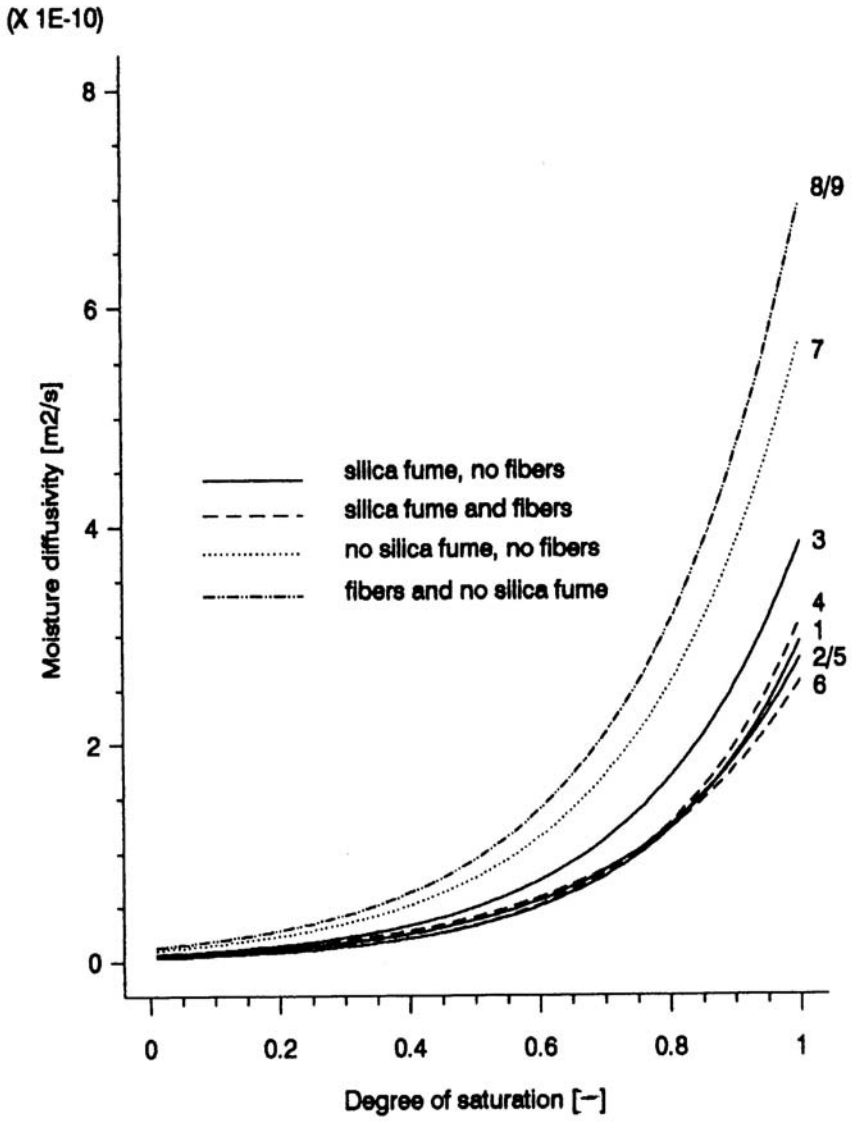

Fig. 7 - Moisture diffusivity of the mortars as a function of the degree of saturation.